



Microstructure and Mechanical Properties of an Al-Mg-Si-Cu Alloy for High Temperature Applications

**H. ADIL^{1*}, F. AUDEBERT^{1,2,3}, F. SAPORITI², S. GERGURI¹,
F. BONATESTA¹ and J. F. DURODOLA¹**

¹School of Engineering, Computing and Mathematics, Oxford Brookes University, Wheatley Campus, OX33 1HX, Oxford, United Kingdom.

²Group of Advanced Materials, Faculty of Engineering, University of Buenos Aires, Paseo Colon 850, Buenos Aires, 1063, Argentina.

³Department of Materials, University of Oxford, 16 Parks Road, OX1 3PH, Oxford, United Kingdom.

Abstract

The high specific properties of aluminium based nanostructured alloys have attracted significant attention due to their promise for structural applications especially at elevated temperatures such as pistons for internal combustion engines. Several types of aluminium-based nanostructured alloys have been developed with microstructures of nanometre-sized particles embedded in the aluminium matrix. In this work a newly developed aluminium based nanostructured alloy is studied to understand its microstructure formation, stability and mechanical properties at elevated temperatures. The microstructure was characterised by means of X-ray diffraction, light and scanning electron microscopies. Heat treatments were carried out to determine the T6 condition properties and the microstructural stability at elevated temperatures for long periods of exposure. The hardness of the new alloy at T6 was 30% higher than the corresponding to Al-4032 which is the commonly used alloy for piston application. The work also compared the mechanical properties of the new alloy with two conventional aluminium alloys used in piston applications. The new alloy has 1.3–4.7 times higher strengths than Al-4032.



Article History

Received: 02 September 2023

Accepted: 24 October 2023

Keywords

Aluminium;
Materials;
Microstructure;
Nanostructured;
Rapid Solidification.

Introduction

Conventional high-strength aluminium alloys are strengthened using various mechanisms

such as grain size refinement, solid solution and others.¹⁻² To meet even higher tensile strength requirements at elevated temperatures; different

CONTACT Habibullah Adil ✉ gma@fi.uba.ar 📍 School of Engineering, Computing and Mathematics, Oxford Brookes University, Wheatley Campus, OX33 1HX, Oxford, United Kingdom.



© 2023 The Author(s). Published by Enviro Research Publishers.

This is an Open Access article licensed under a Creative Commons license: Attribution 4.0 International (CC-BY).

Doi: <http://dx.doi.org/10.13005/msri/200303>

strengthening techniques have been considered to produce nanostructured aluminium based alloys.³⁻⁴ A number of techniques such as mechanical alloying (MA), severe plastic deformation (SPD) and others have emerged over the last two-three decades for processing metals and alloys in a bulk form with the primary aim of grain refinement. A grain size of below 1 μm or less than 100 nm can be achieved with these techniques. It has been reported recently that such nanostructuring of the aluminium alloys not only improves the mechanical properties, but also improves the chemical and service properties.⁵ Several types of aluminium-based nanostructured alloys have been developed with the microstructures of nanometre-sized particles embedded in the aluminium matrix.⁶⁻⁸

Nanostructured (NS) aluminium alloys have attracted significant attention during the last two-three decades due to their high specific mechanical properties compared to conventional aluminium alloys hence offer interesting possibilities related to many structural applications.⁶⁻⁷ The specific properties of interest include higher strength/modulus, lower density and higher temperature capabilities.⁹ NS materials owe their superior properties to their unique microstructure in which the volume of grain boundary is significant, i.e. a 5 nm material has approximately 50% of its volume as grain boundaries.¹⁰ Interest in these new materials is evident from the nearly 3000 research publications and 300 US patents that appeared since 1991 till 2001.¹¹ US government has spent more than \$20 million in funding work to develop and commercialise NS materials through Small Business Innovation Research and Technology Transfer programs.¹¹

It is well known that grain size can be controlled by controlling the rate of solidification from liquid phase. The alloy investigated in this work was produced by a rapid solidification process called melt spinning. Since the introduction of rapid solidification of metallic melts by Duwez in 1960, many techniques and devices have been developed to produce alloys by rapid solidification. These techniques are generally classified into three categories: spray, surface and chill methods. A feature of chill methods is the production of a thin section of liquid metal that is cooled by a larger chill block. Among the chill block methods, the melt spinning is the most widely used

method because of its relatively high cooling rates of up to 10^6 K/sec and suitability for high volume industrial manufacturing. In fact, the accelerated development of rapid solidification technology is due to this technique.¹²⁻¹³ Other advanced methods such as mechanical alloying (MA) and powder metallurgy (PM) are reported to be more successful for refining microstructure of the materials, but are more expensive than rapid solidification.¹⁴⁻¹⁵

In this work a new nanostructured Al-Mg-Si-Cu alloy is studied to understand its microstructure formation and thermal-stability. The mechanical properties of the alloy at elevated temperatures were determined. The work also compares mechanical properties of the new alloy with some conventional aluminium alloys.

Al-Mg-Si-Cu Alloy and Experimental Procedure

The Al-Mg-Si-Cu alloy characterised in this work is produced by rapid solidification process (RSP) [16] using melt spinning production method followed by hot extrusion. The nominal composition of the alloy specified by the manufacturer was AlMg13.5Si7Cu2 wt% and was provided as an extruded bar of 60 mm diameter. RSP Technology Ltd (Company) has been working with F1, Nascars and others since 2001 and has developed a piston alloy line offering a well-balanced compromise of properties. The alloy investigated in this work is named as RSA-612 by the manufacturer; it offers lower density, wear, thermal expansion and increased stiffness & fatigue life. The alloy has good ductility, shape retention during operation and machinability.¹⁶

A sample slice of 8 mm thickness was cut from the bar and prepared for microstructural examinations using grinding and polishing. The sample was later further cut into 8x8x8 mm portions for heat treatments once the as-received material was characterised.

The microstructure was characterised using light and scanning electron microscopes. Light microscope was used for particle analyses while elemental energy dispersive spectroscopy (EDS) and fractographic analyses were carried out using JEOL scanning electron microscope.¹⁷ X-ray diffraction (XRD) analyses were carried out at the Department of Materials, University of Oxford.

In order to optimise the mechanical properties of the as-received alloy, heat treatment studies were conducted to determine the T6 condition, where the material has the optimum strength. Isothermal heat treatments at different temperatures were carried out to assess the alloy's stability when exposed to elevated temperatures for long periods of time.

The mechanical properties at elevated temperatures were investigated by tensile tests at various temperatures. The tests were carried out at the University of Buenos Aires using Interactive Instruments Model 1K Universal Material Tester. All the tensile test specimens were stabilised at the

relevant test temperatures for 100 hours prior to testing. The test specimens were cut perpendicular to the extrusion direction (ED) and all the tests were carried out at strain rate of 10^{-4} s^{-1} .

Results

Microstructural Characterisation

The alloy was characterised using light and scanning electron microscopes. Light microscope was used to observe the microstructural homogeneity, determine particle volume fraction, particle size and distribution. The homogeneity of the alloy was also tested by hardness tests across the sample's cross section.

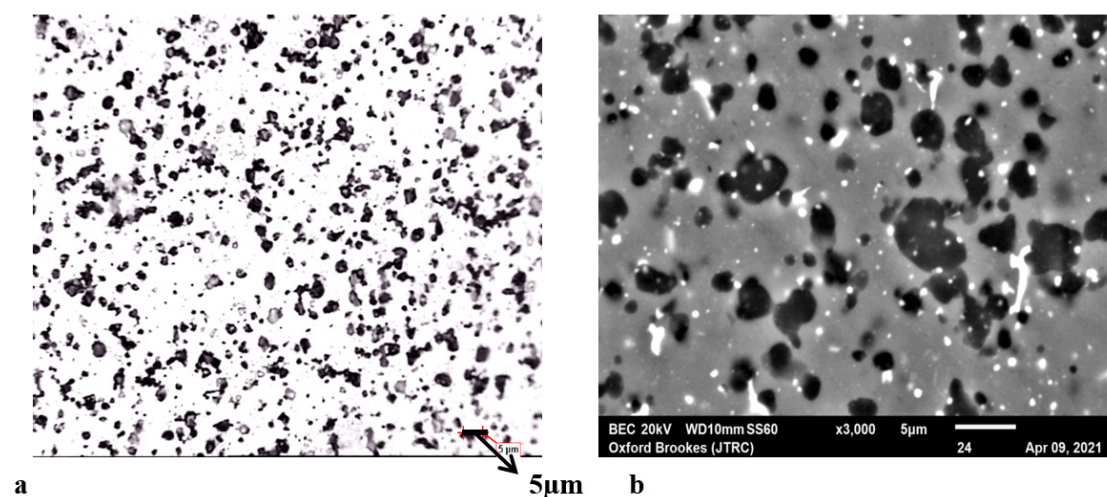


Fig. 1: Images of the microstructure of the alloy in the as-received condition (a) optical micrograph (b) back scattered electron image

Figures 1a and 1b show pictures of the microstructure taken with light and electron microscopes respectively. The light regions are Aluminium matrix and the dark regions are Mg-rich particles or voids where the particles have been dislodged by sample polishing process. The very bright regions in Figure 1b is Copper.

Particle volume fraction analyses were used to confirm the volume fraction as 22.5%. The 3D particle sizes were determined using equations from.¹⁸ The 3D particle sizes of all the observed particles vs. frequency results are presented in Figure 2 and it can be seen that nearly 50% and 90% of the particles have sizes of up to 1.7 and 3.5 μm respectively.

The XRD results, Figure 3 indicate that three different phases were present in the specimens, the most dominant being the Al (α) with the widest peak. The other two phases were Mg_2Si and $\text{Mg}_{17}\text{Al}_{12}$.

Vicker's hardness tests were carried out across the sample's cross section to confirm the results of the particle analyses. The load used for hardness test was 10 Kg at the point of indentation. The hardness along the sample's cross section did not fluctuate significantly therefore signifying the homogeneity of material.

Effect of Heat Treatments

In this work, two types of heat treatments were carried out as outlined in the following sections. Hardness

tests were carried out on the heat treated samples as a mean of determining the effects of different heat treatment conditions on the alloy. Furthermore, two repetitions of the hardness tests were carried out on each heat treated sample. The first test was carried out as the sample was removed from the furnace

and quenched and the other time, on the same sample after leaving it at room temperature (RT) for a week. This was to observe if any major changes occurred in the hardness of the alloy with time after the completion of heat treatments.

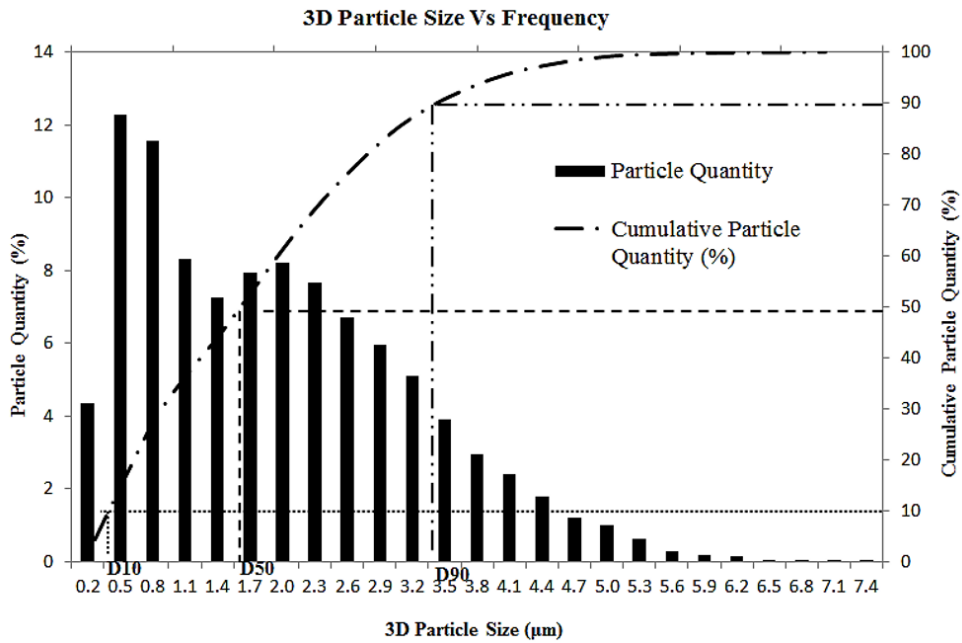


Fig. 2: Particle distribution of all the observed particles.

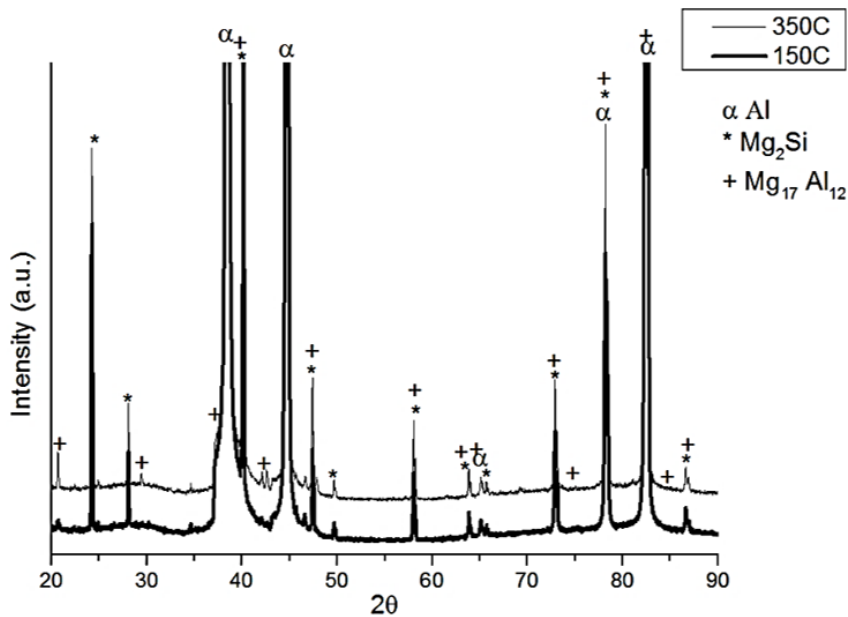


Fig. 3: Diffractograms of the specimens in two different heat treatment conditions

Heat Treatment for T6 Condition

The artificial aging heat treatment hardness test results for the T6 condition are given in Figures 4

and 5. Heat treatments studies were carried out to increase the hardness and strength of the alloy.

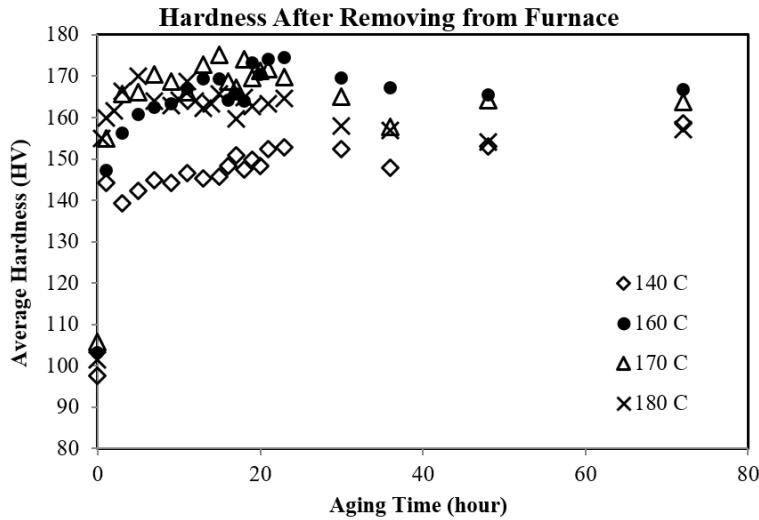


Fig. 3: Diffractograms of the specimens in two different heat treatment conditions

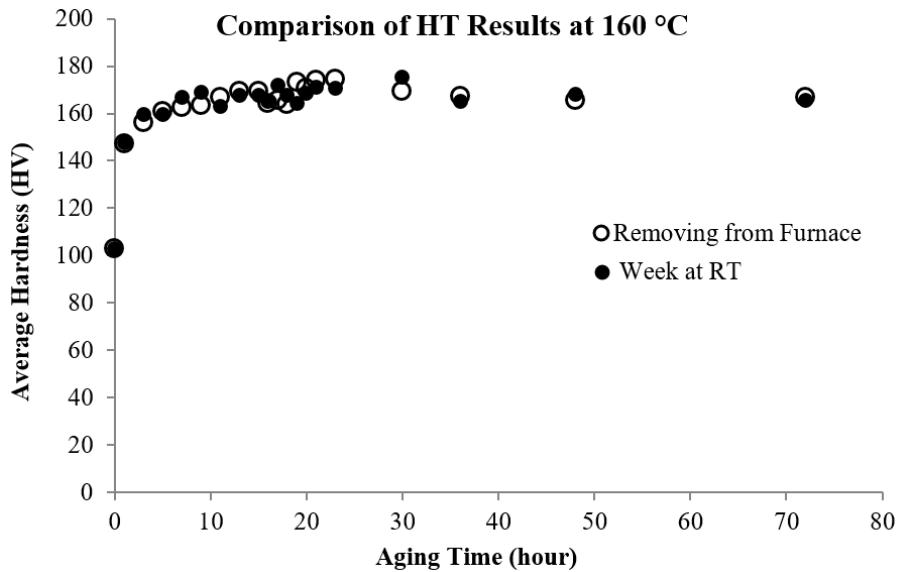


Fig. 5: Comparison of the heat treatment results at 160 °C a week after removing the samples from furnace and just after removing from the furnace

Isothermal Heat Treatments for Microstructural Stability

Microstructure of a heat treatable alloy is time and temperature dependent. This can cause inconsistencies in high temperature tensile test results

since the microstructure undergoes changes during the tensile tests. To avoid this, the microstructure needed to be in a stable state which was achieved through isothermal studies. This involved soaking of the alloy at relevant temperatures at which the

tensile tests would be carried out for long enough time until the microstructure did not change anymore.

The hardness test results for microstructural stability analysis are presented in Figure 6.

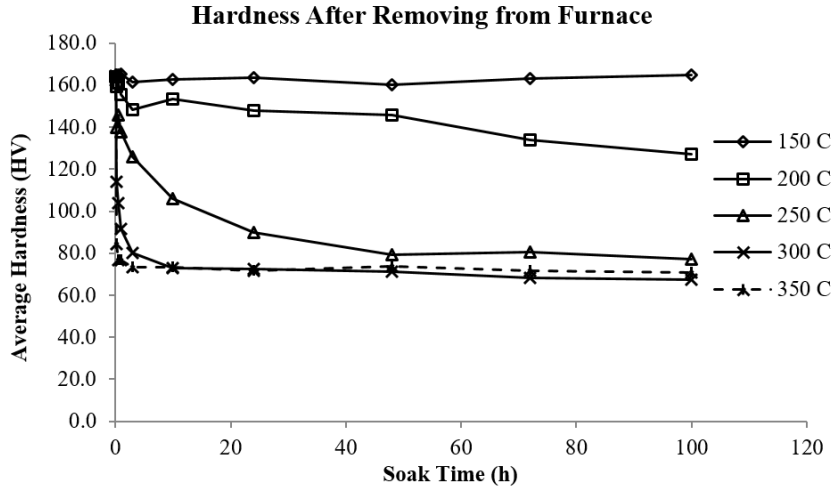


Fig. 6: Microstructural stability heat treatment results

Results of Mechanical Testing

In order to obtain the mechanical properties of the alloy, tensile and compression tests at strain rate of 10^{-4} s^{-1} were carried out. Furthermore, fracture analyses were performed to determine the failures modes.

Tensile Tests

Tensile Test Results

The high temperature tensile tests were carried out at temperatures varying from room temperature

up to 350 °C and the results are presented in Figure 7. The horizontal axis of the graph is offset by 0.05 for each temperature from the previous temperature to better visualise the results at each temperature else the lines falls on top of each other especially at temperatures 200 °C and lower. The data past yield points or plastic region has been cut off and not shown in Figure 7 as it was not of an interest in this work.

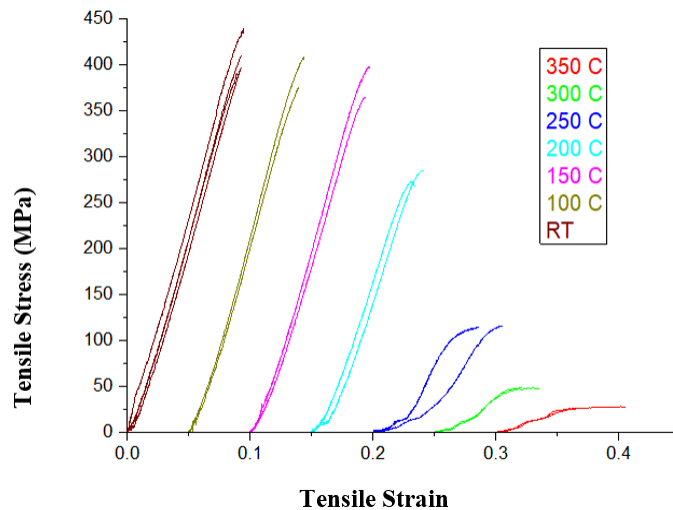


Fig. 7: Tensile test results at several different temperatures

Fracture Analysis of Tensile Test Specimens

Fracture analyses were carried out on the tensile test specimen to determine the cause/mode of failures. The SEM images in Figures 8a and 8b show the

fractured tensile test specimens surfaces at different heat treatment conditions. The analyses show that room temperature sample failed in brittle manner while the 350 °C sample failed in ductile manner.

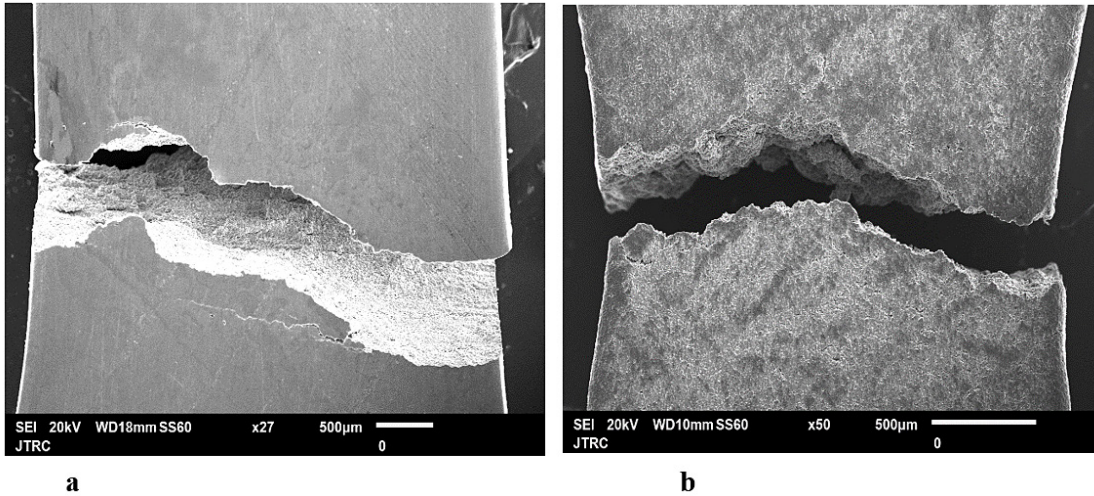


Fig. 8: SEM images of the fractured specimens tested at a) RT (T6) and b) 350 °C

The SEM images of the fractured faces of the test specimens at two different heat treatment conditions are presented in Figures 9a and 9b. Large particles made of Al, Mg and Si were observed in the fractured

faces with pits around them. The EDS spectrums of these large particles for the test specimens at RT and 350 °C are presented.

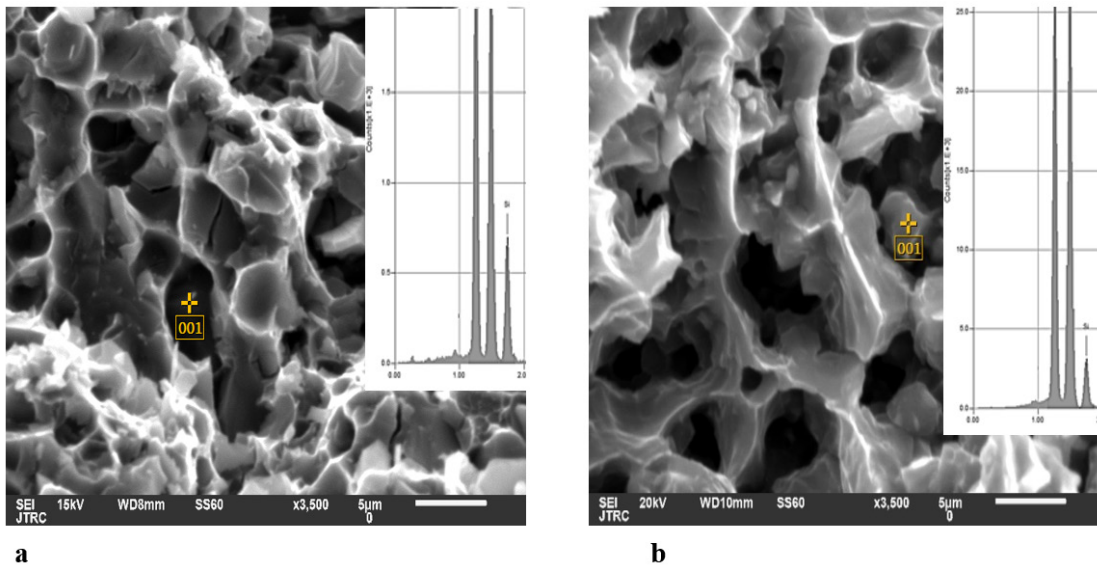


Fig. 9: SEM image of the fracture face of the specimen tested at (a) room temperature (T6) (b) 350 °C

Compression Tests

Compression Test Results

The compression tests were carried out on specimens cut from the bar in extrusion direction (ED) and 90° degree to the ED, called transverse (Tran) direction. The compression test results were plotted in Figure 10. The average yield strengths in the extrusion and transverse directions are approximately 550 and 510 MPa respectively.

Fracture Analyses of Compression Test Specimens

Fracture analyses of the compression test specimens showed that pitting occurred around large particles Figures 11a and 11b which could have led to the initiation of cracks. The large particles mainly consisted of Al, Mg and Si as can be seen in Figures 11a and 11b.

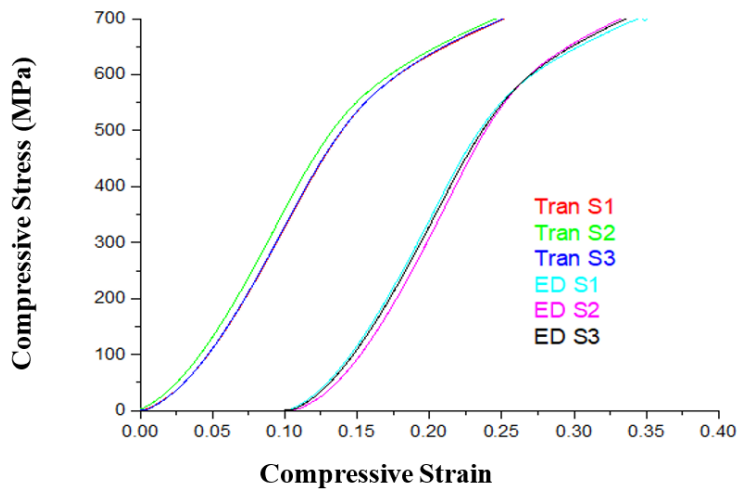


Fig. 10: Compression test results of the new alloy for the specimens cut from the extruded bar in two different directions

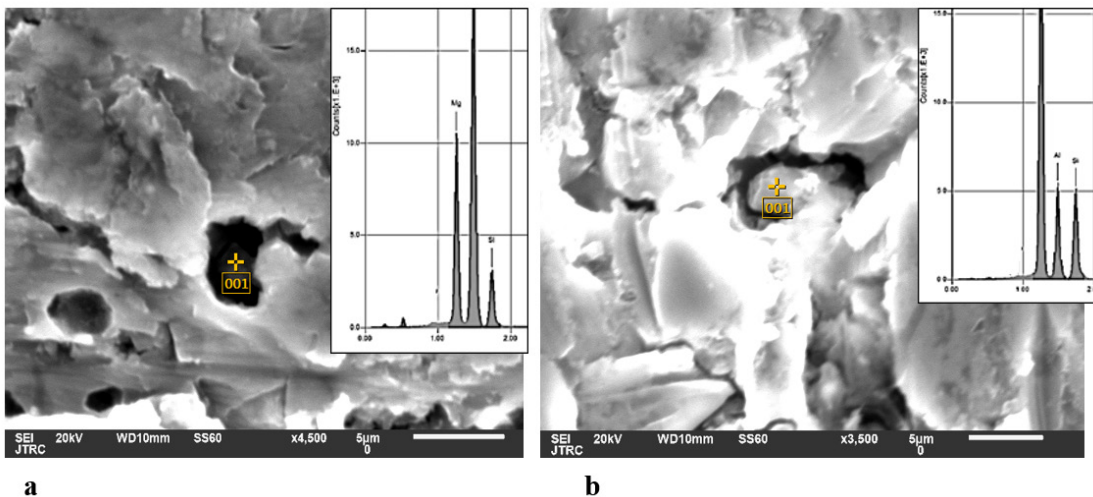


Fig. 11: SEM image of the fracture face of the specimen in (a) extrusion b) transverse directions

Strength Contribution of different Strengthening Mechanisms

Pedrazzini *et al.*¹⁸ discussed the contribution of different strengthening mechanisms to the yield

strength of an aluminium based nanostructured alloy ($Al_{93}Fe_3Cr_2Ti_2$). Similar approach has been used in this work.

Particle Strengthening

Orowan mechanism which accounts for dislocation bowing around particles is the more common strengthening mechanism in alloys such as the one investigated in this work. Its contribution to the yield strength can be estimated by equation (1)¹⁹

$$\Delta\sigma_p = M \frac{G \cdot b}{L} \quad \dots(1)$$

Where $\Delta\sigma_p$ (GPa) is the strengthening contribution to yield stress due to the hard particles, M is the Taylor factor that accounts for the homogeneous deformation of the individual grains in a polycrystal, G is the shear modulus (27 GPa for aluminium), b is the Burgers vector (0.286 nm),²⁰ and L is the edge to edge planar inter-particle spacing (nm) for the spherical particles that can be estimated using equation (2)¹⁹

$$L = \frac{2 \cdot D_s}{3 \cdot f_v} (1 - f_v) \quad \dots(2)$$

Where f_v is particle volume fraction (22.5%) and D_s is the mean planar particle diameter, which is related to the particle diameter in volume, D_p as in equation (3).¹⁹

$$D_s = D_p \sqrt{(2/3)} \quad \dots(3)$$

For an aluminium based nanostructured alloy (Al-Cu),¹⁹ estimated the precipitate diameter (D_p) to be 110 nm. This value was assumed for this alloy.

M in equation (1) is dependent on the matrix texture and therefore different values are reported in literature, but for an aluminium based hot extruded nanostructured alloy ($Al_{93}Fe_3Cr_2Ti_2$), a value of 3.5 has been adopted,^{18, 19} in this works.

Using equations (2) and (3) gives equation (4).

$$\Delta\sigma_p = M \frac{G \cdot b}{\frac{2 \cdot D_p \sqrt{\frac{2}{3}}}{3 \cdot f_v} (1 - f_v)} \quad \dots(4)$$

Substituting the above values into equation (4) gives a value of 131 MPa. This is about 32% of the alloy's strength which aligns with values reported in literature.¹⁸

Grain Boundary Strengthening

Grain boundary strengthening can be estimated by the Hall-Petch (H-P) equation, as shown in equation (5), which has been found to match quantitatively the grain size effect on the yield strength of polycrystalline materials.^{19, 21}

$$\Delta\sigma_{gb} = \sigma_0 + k/\sqrt{d} \quad \dots(5)$$

Where $\Delta\sigma_{gb}$ (MPa) is the strengthening contribution to yield stress due to the grain boundaries, σ_0 is the lattice frictional stress (for Al, it is commonly taken as $\sigma_0 = 16$ MPa), d is the average grain size, and k, is known as the "locking parameter", which measures the relative hardening contribution of the grain boundaries.

For an aluminium based nanostructured alloy (Al-Cu),²⁰ estimated the average grain size (d) and locking parameter (k) to be 30 nm and 0.13 MPa \sqrt{m} respectively.

Substituting the above values into (6) estimates that nearly 55.5 MPa which is about 13.6% of alloy's strength.

Dislocation-Dislocation Interaction Strengthening

Dislocation-dislocation interaction is an important strengthening mechanism to be considered here and it can be estimated using equation (7)¹⁹

$$\Delta\sigma_d = M \cdot \alpha \cdot G \cdot b \cdot \sqrt{\rho} \quad \dots (7)$$

Where $\Delta\sigma_d$, M, α , G, b and ρ are strengthening contribution to yield stress due to the dislocation-dislocation interaction, Taylor factor, dislocation strengthening efficiency, shear modulus, Burger vector and dislocation density.

Dislocation strengthening efficiency is a function of the strain rate and temperature, and at strain rate of 10^{-4} s⁻¹ and room temperature, it is reported to be 0.3. According to [19], a reasonable dislocation density value for hot extruded nanostructured alloy is of the order of 10^{14} m⁻².

Substituting these values into (7) estimates that nearly 81 MPa or 19.8% of alloy's strength was

contributed by dislocation-dislocation interaction. This aligns with values reported in literature.¹⁹

Solid Solution Strengthening

Considering the high solubility of the alloying elements in this alloy facilitated by rapid solidification method melt spinning, the remaining strength 141 MPa or 34.6% was assumed to be contributed by the solid solution strengthening.

Discussion

Microstructure of the Alloy

The particles sizes were many folds smaller compared to the aluminium alloys produced using industrial metallurgy (IM) methods where the sizes of particles vary 10 – 100 μm .¹⁵ The smaller size of particles can be ascribed to the rapid solidification (RS) method melting spinning used to produce the alloy investigated in this work.²²

The results in Figure 2 show that there is significant variation in particle sizes across the cross section of the bar. The actual particle sizes were likely to be smaller than measured because some of the particles dislodged from the aluminium matrix during grinding and polishing the sample. The voids left which were measured were expected to be larger than the particles. The particle analyses results indicated uniform particle distribution which resulted in uniform mechanical properties as confirmed by the hardness tests results across the cross section of the bar.²²

The X-ray diffraction (XRD) analyses Figure 3 determined the presence of three different phases with the most dominant being Al (α), while the other two were Mg_2Si and $\text{Mg}_{17}\text{Al}_{12}$ and both of them are known to improve not only strength of the alloy, but other properties such as wear, corrosion and ductility²³⁻²⁴

Heat Treatments

It is not straight forward to determine the T6 condition from the artificial aging heat treatments results in Figures 4 and 5 because the results overlap. However, the aging results at 160 °C follow the theoretical curve pattern for T6 condition Figure 5, which increases incrementally reaching a maximum and then slowly decreases. Furthermore, the hardness of the sample heat treated at 160 °C for 30 hours did not change significantly after removal from

the furnace and leaving it at RT for a week, Figure 5. This appears to correspond to a T6 condition. The hardness of the new alloy increased from an average of 97 HV in as-received state to 175.5 HV at T6 condition.

The samples soaked at different temperatures reached stability at different lengths of times; however the samples at 200 °C took the longest, 100 h to reach stability, Figure 6. While the samples treated at 150 °C did not reflect any impact on the hardness at all, indicating that no significant microstructural changes occurred in the alloy up to 150 °C. The alloy reached thermal stability at approximately 100 hours for all temperatures.

Mechanical Properties, Deformation and Fracture Behaviour

It can be seen from the tensile tests results in Figure 7 that the specimens in room temperature or T6 condition have the highest yield strengths with an average value of approximately 409 MPa, but show no appreciable elongation. On the other hand, the specimens at 350 °C had the lowest strengths with an average value of approximately 26 MPa, but had the highest elongation. The results also indicated that the alloy did not show any significant reduction in strength up to 150 °C similar to stability results in Figures 6 which could be due to the lack of coarsening of the strengthening particles.¹⁵ Furthermore, there was no significant scatter in test results for different specimens in the same testing conditions because the test specimens were stabilised prior to testing.

Fracture analyses of tensile test specimen, tested at room temperature shows of brittle failure, no necking can be observed, Figure 8a. While a specimen tested at 350 °C had appreciable necking and failed in ductile manner, Figure 8b. Furthermore, the specimen tested at RT fractured approximately 45° to the applied load while the specimen tested at 350 °C fractured 90° to the applied load, showing the fracture was caused by normal stress.

Fractographic analyses of samples, Figures 9a and 9b showed that large particles made of Al, Mg and Si respectively form pits around them and could have been the likely cause of fracture/crack initiation. The average dimple sizes were 3.8 and 5.4 micron for samples tested at RT and 350 °C respectively.

In addition, the fracture surface of the specimen tested at T6 state, Figure 9a, did not show any appreciable microplasticity compared to the specimen tested at 350°C, Figure 9b. The microplasticity at 350°C could be due to the aluminium matrix becoming soft and flows. Furthermore, there were more micro-cracks in the specimen tested in T6 state than the specimen tested at 350°C; this could be due to the lack of microplasticity, indicating that the aluminium matrix has been sheared.

The compression test results shown, Figure 10, demonstrated that the specimens in extrusion direction (ED) had higher yield strengths compared to the transverse direction. This is because of the grains alignment along the extrusion direction.²⁷⁻²⁸ Furthermore, the average yield strength in transverse direction was approximately 510 MPa which was 25% higher compared to 409 MPa in tension.

Fractographic analyses of the specimens tested in compression also revealed that pitting occurred around large particles, Figures 11a and 11b; that were made of Al, Mg and Si.

The tensile test results obtained in Section 3.3.1.1 for the new alloy showed an improvement over other conventional aluminium alloys at the test temperatures. Figure 12 compares the yield strengths of the new alloy and two conventional aluminium alloys used in high temperature applications, specifically pistons. It can be seen that the new alloy has higher yield strengths at test temperatures than the conventional aluminium alloys. This opens opportunity for high temperature applications such as in internal combustion engine components. The yield strength values for the conventional alloys were obtained from.²⁵⁻²⁶

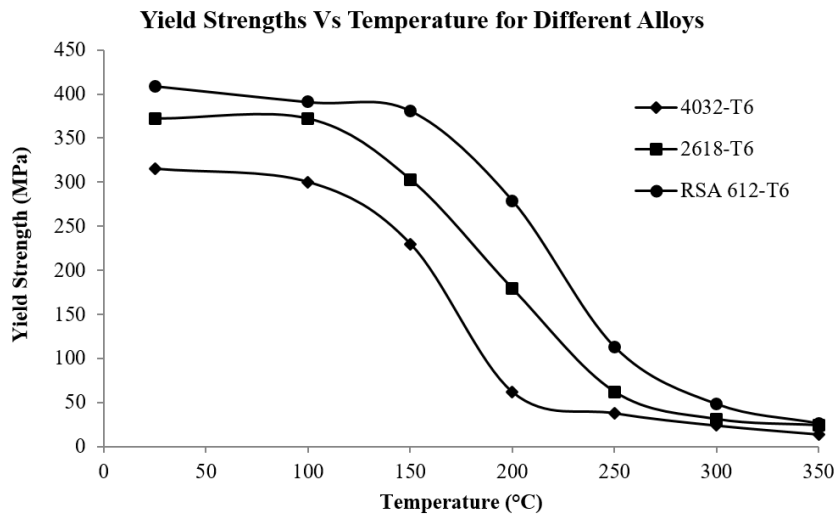


Fig.12: Yield strength comparison of two different aluminium alloys vs. the new alloy.²⁵⁻²⁶

Conclusion

A newly developed aluminium based nanostructured alloy was investigated in this work to understand its microstructure formation and determine the mechanical properties. Microscopic analyses showed a homogenous microstructure which leads to homogenous mechanical properties, a highly desired property in component design. The T6 condition was 30 hours at 160 °C and the alloy's hardness increased from 97 HV on average in as received state to 175.5 HV in T6.

Tensile tests showed that the alloy had yield strength of 409 and 26 MPa at room temperature and 350 °C respectively. The new alloy had 1.3–4.7 times higher strengths than Al-4032 which is the commonly used alloy for piston application. Furthermore, there was insignificant scatter in the tensile test results indicating homogenous microstructure.

Fractographic analyses of the test specimens revealed that large particles made of Al, Mg and

Si form pits around them which could have been the likely cause of crack initiation due to thermal mismatch between aluminium matrix and the particles.

The different strengthening mechanisms that contributed to the strength of the new alloy were estimated to be 34.6% 32%, 19.8%, 13.6%, solid solution strengthening, particle strengthening, dislocation-dislocation interaction and grain size strengthening.

Acknowledgements

The authors would like to thank RSP Technology for the provision of the alloy used in this work.

Funding

The author(s) received no financial support for the research, authorship, and/or publication of this article.

Conflict of Interest

The authors do not have any conflict of interest.

References

- Callister Jr WD, Rethwisch DG. Callister's materials science and engineering. John Wiley & Sons; 2020 Feb 5.
- Embury JD, Lloyd DJ, Ramachandran TR. Strengthening mechanisms in aluminum alloys. *In Treatise on Materials Science & Technology* 1989 Jan 1 (Vol. 31, pp. 579-601). Elsevier.
- Asgharzadeh H, Simchi A, Kim HS. A plastic-yield compaction model for nanostructured Al6063 alloy and Al6063/Al₂O₃ nanocomposite powder. *Powder technology*. 2011 Aug 10;211(2-3):215-20.
- Inoue A, Kimura H, Amiya K. Developments of aluminum-and magnesium-based nanophase high-strength alloys by use of melt quenching-induced metastable phase. *Materials transactions*. 2002;43(8):2006-16.
- Sabirov I, Murashkin MY, Valiev RZ. Nanostructured aluminium alloys produced by severe plastic deformation: New horizons in development. *Materials science and engineering: A*. 2013 Jan 10;560:1-24.
- Audebert F, Mendive C, Vidal A. Structure and mechanical behaviour of Al-Fe-X and Al-Ni-X rapidly solidified alloys. *Materials Science and Engineering: A*. 2004 Jul 1;375:1196-200.
- Galano M, Audebert F, Escorial AG, Stone IC, Cantor B. Nanoquasicrystalline Al-Fe-Cr-based alloys with high strength at elevated temperature. *Journal of Alloys and Compounds*. 2010 Apr 16;495(2):372-6.
- Galano M, Audebert F, Cantor B, Stone I. Structural characterisation and stability of new nanoquasicrystalline Al-based alloys. *Materials Science and Engineering: A*. 2004 Jul 1;375:1206-11.
- Lewis RE, Fitzpatrick JM, Crooks DD, Singer AR, Jenkins WN. A novel approach for rapid solidification processing of high strength PM aluminum alloys. *SAE transactions*. 1984 Jan 1:357-63.
- Han BQ, Mohamed FA, Lavernia EJ. Tensile behavior of bulk nanostructured and ultrafine grained aluminum alloys. *Journal of materials science*. 2003 Aug;38(15):3319-24.
- Tellkamp VL, Lavernia EJ, Melmed A. Mechanical behavior and microstructure of a thermally stable bulk nanostructured Al alloy. *Metallurgical and Materials Transactions A*. 2001 Sep;32(9):2335-43.
- Uzun O, Karaaslan T, Keskin M. Production and structure of rapidly solidified Al-Si alloys. *Turkish Journal of Physics*. 2001 Aug 1;25(5):455-66.
- Abed EJ. Rapidly solidified of hyper eutectic aluminum-silicon alloys ribbons by using melt-spinning techniques. *International Journal of Current Engineering and Technology*. 2014;4(3):1394-8.
- Zuo M, Liu XF, Sun QQ, Jiang K. Effect of rapid solidification on the microstructure and refining performance of an Al-Si-P master alloy. *Journal of Materials Processing Technology*. 2009 Aug 1;209(15-16):5504-8.
- Lobry P, Błaż L, Sugamata M, Kula A. Effect of rapid solidification on structure and mechanical properties of Al-6Mn-3Mg alloy. *Archives of Material Science and Engineering*. 2011 Jun;49(2):97-102.
- https://www.rsp-technology.com/sitemedia/useruploads/rsp_alloys_overview_2018lr.pdf
- https://www.jeol.co.jp/en/products/detail/JSM-6010PLUS_LA.html

18. Pedrazzini S, Galano M, Audebert F, Collins DM, Hofmann F, Abbey B, Korsunsky AM, Liebllich M, Escorial AG, Smith GD. Strengthening mechanisms in an Al-Fe-Cr-Ti nano-quasicrystalline alloy and composites. *Materials Science and Engineering: A*. 2016 Aug 30;672:175-83.
19. Galano M, Audebert F. Novel Al based Nanoquasicrystalline Alloys. *Progress in Materials Science*. 2021 Jun 16:100831.
20. Shanmugasundaram T, Heilmaier M, Murty BS, Sarma VS. On the Hall–Petch relationship in a nanostructured Al–Cu alloy. *Materials Science and Engineering: A*. 2010 Nov 15;527(29-30):7821-5.
21. Eshelby JD, Frank FC, Nabarro FR. XLI. *The equilibrium of linear arrays of dislocations. The London, Edinburgh, and Dublin Philosophical Magazine and Journal of Science*. 1951 Apr 1;42(327):351-64.
22. Rafiei A, Varahram N, Davami P. Microstructural study of Al-20Si-5Fe Alloys produced by melt-spinning. *Metallurgical and Materials Engineering*. 2013 Mar 31;19(1):85-94.
23. Asghar, Ghulam, Liming Peng, Penghuai Fu, Lingyang Yuan, and Yue Liu. "Role of Mg₂Si precipitates size in determining the ductility of A357 cast alloy." *Materials & Design* 186 (2020): 108280.
24. Moharami, A., A. Razaghian, B. Babaei, O. O. Ojo, and M. Šlapáková. "Role of Mg₂Si particles on mechanical, wear, and corrosion behaviors of friction stir welding of AA6061-T6 and Al-Mg₂Si composite." *Journal of Composite Materials* 54, no. 26 (2020): 4035-4057.
25. Kaufman JG, editor. Properties of aluminum alloys: tensile, creep, and fatigue data at high and low temperatures. *ASM international*; 1999.
26. American Society for Metals. Handbook, C. (1979) Metals handbook. Vol.2, Properties and selection: nonferrous alloys and pure metals, 9th ed. *Metals Park: American Society for Metals*.
27. Chen Y, Clausen AH, Hopperstad OS, Langseth M. Stress–strain behaviour of aluminium alloys at a wide range of strain rates. *International Journal of Solids and Structures*. 2009 Oct 15;46(21):3825-35.
28. Wang H, Boehlert CJ, Wang QD, Yin DD, Ding WJ. In-situ analysis of the tensile deformation modes and anisotropy of extruded Mg-10Gd-3Y-0.5 Zr (wt.%) at elevated temperatures. *International Journal of Plasticity*. 2016 Sep 1;84:255-76.